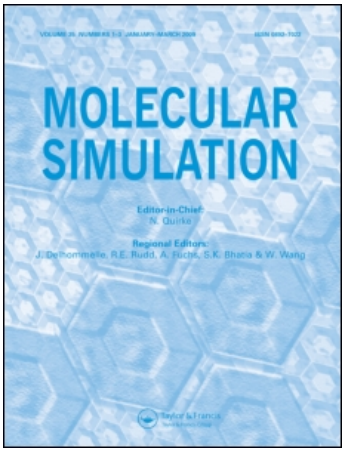

Molecular Simulation
Publication details, including instructions for authors and subscription information:
http://www.informaworld.com/smpp/title~content=t713644482

Grand Canonical Monte Carlo Simulation for Solubility Calculation in Supercritical Extraction

M. Nouacer[a]; K. S. Shing[a]
[a] Department of Chemical Engineering, University of Southern California, Los Angeles, California, USA

To cite this Article Nouacer, M. and Shing, K. S.(1989) 'Grand Canonical Monte Carlo Simulation for Solubility Calculation in Supercritical Extraction', Molecular Simulation, 2: 1, 55 — 68
To link to this Article: DOI: 10.1080/08927028908032783
URL: http://dx.doi.org/10.1080/08927028908032783

Molecular Simulation, 1989, Vol. 2, pp. 55–68
Reprints available directly from the publisher
Photocopying permitted by license only

GRAND CANONICAL MONTE CARLO SIMULATION FOR SOLUBILITY CALCULATION IN SUPERCRITICAL EXTRACTION

M. NOUACER and K.S. SHING

Department of Chemical Engineering, University of Southern California, Los Angeles, California 90089-1211, USA

(*Received January 1988; in final form April 1988*)

The Grand Canonical Ensemble Monte Carlo (GCEMC) technique is used to simulate highly nonideal dilute mixtures in the near vapor-liquid critical region. These systems are commonly found in supercritical fluid extraction processes. Mixtures composed of model CO_2/naphthalene/water molecules are studied. Very large and highly correlated concentration fluctuations were observed. It was found that when the total number of molecules in the system exceeded about 150, system size dependence was not significant. The GCEMC method breaks down when the system density exceeds about 1.5 times the solvent critical density due primarily to the low probability of successful addition and removal of the large naphthalene molecules. In some systems, the presence of a small amount of water caused a dramatic increase in the system density and in naphthalene solubility. By examining the radial distribution functions in these mixtures, the origin of this effect can be attributed to the preferential aggragation of the solute naphthalene molecules around the highly polar water molecules.

KEY WORDS: Grand Canonical Ensemble, Monte Carlo, supercritical extraction, dilute mixtures, solubility.

1. INTRODUCTION

Supercritical extraction is an industrial separations process in which a compressed gas solvent above its critical point is used to selectively extract certain components from a condensed phase, which may be a solid or liquid mixture [1]. In this work, we are particularly interested in the case in which the condensed phase is a solid. Since the solvent gas can be assumed to be insoluble in the solid, the chemical potential of any solid solute in the supercritical solvent phase is equal to that of the pure solid solute at the extraction pressure and temperature. The density of the supercritical phase is usually less than normal liquid densities because of the high cost associated with very high pressure operations. To better understand the relationship between solubilities and molecular characteristics of solute and solvent, we have previously use the NpT ensemble to study these systems [2]. The NpT ensemble, however, does not allow specification of the chemical potentials and also suppresses concentration fluctuations, which are important in the near critical region. Therefore, the Grand Canonical Ensemble Monte Carlo (GCEMC) method appears to be an attractive and ideal technique to use for these systems. Our purpose in conducting this study is two-fold: first, to examine the general applicability and behavior of GCEMC in the near vapor-liquid critical region for highly nonideal mixtures. The second objective is to examine the thermodynamic behavior of typical supercritical fluid extraction (SFE) systems in this region of the phase diagram.

The effect of adding a trace amount of water is also studied. This is of interest because in some experimental studies, the addition of highly polar components resulted in greatly increased solubilities and hence extraction efficiencies [3]. The physical origin of this effect is best studied using molecular simulation because molecular simulation provides structural information in the form of distribution functions which shed light on such pheonomena as preferential molecular aggregation.

The model mixture we chose to study is a naphthalene-like large hydrocarbon solute dissolved in CO_2, a typical SFE solvent. This is the same mixture we studied previously using the NpT ensemble, so comparisons can be made.

2. THEORY AND SIMULATION METHOD

2.1 The Algorithm

When a solid solute (assumed pure) coexists in equilibrium with a supercritical solvent containing some of the solute, the chemical potential of the solute is equal in both phases, i.e.,

$$\mu_1^{cS} = \mu_1^{cF} \tag{1}$$

where μ_1^{cS} and μ_1^{cF} are the configurational chemical potentials of the solute (component 1) in the solid and supercritical fluid phases, respectively. μ_1^{cS} is a known function of temperature (T) and pressure (P), whereas μ_1^{cF} is a function of T, P and composition. The GCEMC method uses the prescribed values of μ_1^{cS}, μ_2^{cF} (solvent chemical potential), T and volume V to calculate the composition (or the solubility).

The GCEMC algorithm used in this work is a straightforward generalization of the one used by Adams [4]. Adopting Adams' notation for the chemical potentials, we define

$$BB_i = \frac{\mu_i^r}{kT} + \ln \langle N_i \rangle = \frac{\mu_i^c}{kT} + \ln (V/\sigma^3) \tag{2}$$

where μ_i^r is the residual chemical potential of component i, and is given by

$$\frac{\mu_i^r}{kT} = \frac{\mu_i^c}{kT} - \frac{\mu_i^{c,ideal}}{kT}. \tag{3}$$

μ_i^c, $\mu_i^{c,ideal}$ are respectively the configurational chemical potential of component i, and that for component i as an ideal gas at the same temperature occupying the same volume V. For the two component case (solute $\equiv$ 1, solvent $\equiv$ 2) the algorithm is as follows.

The temperature T, volume V and BB_1 and BB_2 are chosen so that the state condition corresponds to a near critical state for the system. A randomly selected molecule is moved and the move is accepted or rejected as in a canonical ensemble simulation. Then, with equal probability, we decide to add or remove one solute or solvent molecule. The removal attempt is accepted with probability

$$\frac{P_{N_i-1}}{P_{N_i}} = N_i \exp\left(-BB_i - \frac{\Delta U}{kT} \right) \tag{4}$$

where P_{N_i} is the probability of finding a configuration with N_i molecules of component i, with energy $U(N_i)$. $\Delta U^- \equiv U(N_i - 1) - U(N_i)$ is the congfigurational energy change due to deletion of a molecule of component i. Here i can be 1 (solute) or 2 (solvent). The addition attempt is accepted with probability

$$\frac{P_{N_i+1}}{P_{N_i}} = \frac{1}{N_i + 1} \exp\left[BB_i - \frac{\Delta U^+}{kT}\right]$$

where

$$\Delta U^+ \equiv U(N_i + 1) - U(N_i). \tag{5}$$

The pressures and internal energies are calculated in the usual way. The volumes are selected so that the average number of molecules in each system is between 100 and 200. The average length of each simulation is 5×10^6 configurations, with each configuration a single attempted move.

2.2 Intermolecular Potential Models

As mentioned previously, we are interested in modelling a large hydrocarbon solute which is naphthalene-like and the solvent is CO_2. One to two molecules of water are added to some mixtures to study the effect of the presence of water. The model pair potentials selected and the values of the parameters are summarized in Table 1.

3. RESULTS AND DISCUSSIONS

In this work, we studied a single isotherm, $kT/\varepsilon = 1.719$, which corresponds to a temperature above the critical temperature of the model CO_2 (estimated to be about

Table 1 Intermolecular potential models and molecular parameters used.

Model	*Interacting pair (a–b)*	ε/k *[°K]*	σ *[Å]*	$Q_A^* Q_B^*$ *[5]*	$\mu_a^* \mu_b^*$ *[6]*	$\mu_a^* Q_b^*$
	CO_2-CO_2	198.00	3.76	0.90		
LJ + QQ	NAPH-NAPH	492.28	5.45	12.02		
	NAPH-CO_2	312.27	4.60	3.29		
LJ + DD	H_2O-H_2O	355.89	2.72		2.33	
LJ + DQ	H_2O-CO_2	265.45	3.24			1.448
	H_2O-NAPH	419.82	4.08			5.292

LJ = Lennard-Jones potential, $\phi_{ab} = 4\varepsilon_{ab}\left[\left(\frac{\sigma_{ab}}{r}\right)^{12} - \left(\frac{\sigma_{ab}}{r}\right)^{6}\right]$

QQ = quadrupole-quadropole interaction, defined as in [7].
DD = dipole-dipole interaction, defined as in [7].
DQ = dipole-quadrupole interaction, defined as in [7].

$\mu\varepsilon_a^* \mu_b^* \equiv \frac{\mu_a \mu_b \sigma^3}{\varepsilon}$, μ_a, μ_b = dipole moments of molecules a and b in the interacting pair a-b.

$Q_a^* Q_b^* \equiv \frac{Q_a Q_b \sigma^5}{\varepsilon}$, Q_a, Q_b = quadrupole moments of molecules a and b in the interacting pair a-b.

$\mu_a^* Q_b^* \equiv \frac{\mu_a Q_b \sigma^4}{\varepsilon}$,

Here ε and σ are those for the CO_2-CO_2 pair potential [8].

$kT_c/\varepsilon = 1.54$). We present results for the following:

i) GCEMC method in the near vapor-liquid critical region,
ii) The size of fluctuations in GCEMC in this region,
iii) The effect of varying the chemical potential of solute BB_1,
iv) The effect of varying the chemical potential of solvent BB_2,
v) The dependence of results on system size V,
vi) The effect of water addition.

All results are reduced with respect to ε and σ, the energy and size parameters of the Lennard-Jones part of the CO_2–CO_2 potential.

3.1 Size of fluctuations in the near critical region

In Figure 1 we show the fluctuations in concentrations $\langle N_1 \rangle$ and $\langle N_2 \rangle$, in the internal energy $\langle U \rangle$ and the pressure for a near-critical density system. We note that the fluctuations in density ($\varrho^* = (N_1 + N_2)\sigma^3/V$) are large, of the order of 12%, and the fluctuations in concentration of solute are much larger than for the solvent (70% versus 12%). This is because the concentration of the solute is low (about 3%) and

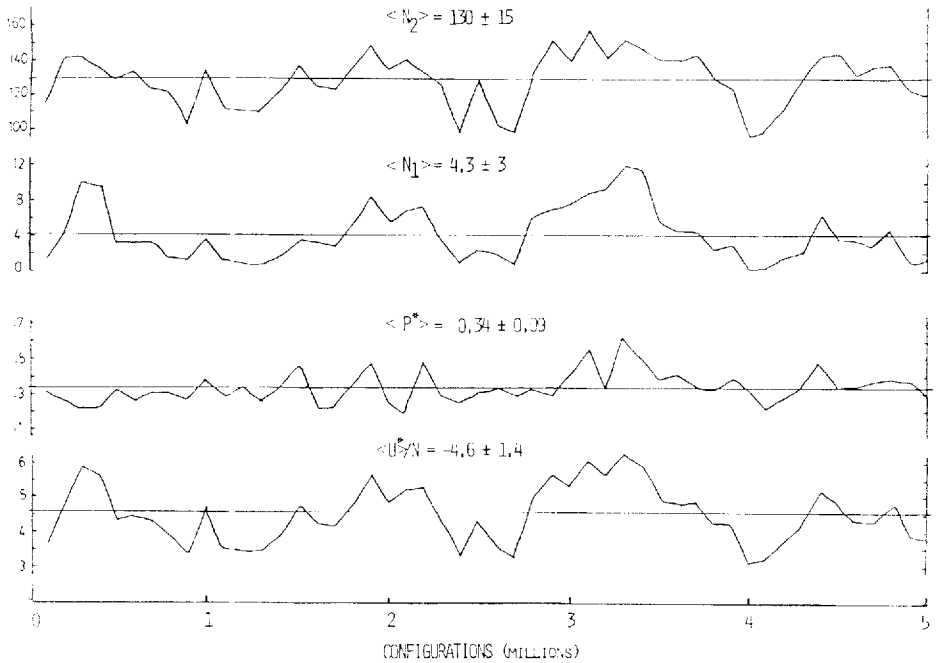

Figure 1 Fluctuations in GCEMC simulations of CO_2/naphthalene mixture in the near vapor-liquid critical region. $kT/\varepsilon = 1.719$, $BB_1 = -5.8$, $BB_2 = 3.35$, $V/\sigma^3 = 305$, $\langle \varrho^* \rangle = (\langle N_1 \rangle + \langle N_2 \rangle)\sigma^3/V = 0.44$. The line indicate subaverages over 1×10^5 configurations. The ensemble averages over the whole simulation are represented by the horizontal straight lines. The quoted uncertainties are root-mean squared deviations of the subaverages from the overall average.

also because the system is close to the vapor-liquid critical point. Since significant deviations from the mean values persist over large numbers of configurations (see for example the subaverages between 3–4 $\times$ 10^6 configurations in Figure 1), meaningful averages cannot be obtained unless the simulations are quite long. We also note that there is almost perfect correlation between the fluctuations of N_1, N_2 (and hence the overall density), and the internal energy. This correlation can be explained in physical terms by noting that an instantaneous increase in the local density due to successive successful additions of either solute or solvent molecules favor further addition of solute molecules since the solubility is approximately an exponential function of density over a large portion of the density range [2]. As a result, increases in N_1 are always accompanied by increases in N_2 and vice versa. This correlation in N_1 and N_2 also leads to accompanying fluctuations in U. The pressure fluctuations are less strongly correlated because pressure does not vary significantly with density in the near-critical region. The behavior shown in Figure 1 is typical of mixtures studied in this work. The size of the fluctuations depends on the mean density; large fluctuations occur at less than the critical density and smaller fluctuations occur above critical density.

3.2 Comparison between GCEMC (μVT) and isothermal-isobaric (NpT) simulation results

We selected two state conditions and performed both NpT and μVT simulations. These two states correspond to a gas-like density of about $\varrho^* = 0.1$ and a near critical density of $\varrho^* = 0.3$. The comprisons are shown in Table 2. We see that the results for NpT and μVT are in agreement, given the statistical uncertainties of the simulations. We also note that small changes in the specified configurational chemical potentials in the μTV simulation resulted in a significant change in the density (changing μ_1^c/kT, μ_2^c/kT from -11.4, -2.69 to -11.7, -2.39 changed the density from 0.119 to 0.38 and $\langle N_1 \rangle$ from 0.044 to 1.61). On the other hand, the residual chemical potentials showed a much larger change between the two densities. The reason for this is that since $\mu_i^c/kT = \mu_i^r/kT + \ln(\varrho^* y_i)$ (i is either 1 or 2 here amd y_i is the mole fraction of i), and μ_i^r decreases with density while $\ln(\varrho^* y_i)$ increases with density (and concentration), these two effects tend to balance each other, leaving μ_i^c/kT only slightly changed. This means that the densities and concentrations are very sensitive to μ_i^c/kT, which are the specified parameters in μVT simulations. As shown in 2.1 the statistical

Table 2 Comparison of NpT and μVT results for two densities

	μVT	NpT	μVT	NpT
V/σ^3	296	947	296	309
μ_i^r/kT	-2.45	-2.56	-6.45	-6.72
μ_1^c/kT	-11.4	*	-11.7	-11.7
μ_2^r/kT	-0.56	-0.51	-1.38	-1.20
μ_2^c/kT	-2.69	-2.69	-2.39	-2.39
$\varrho\sigma^3$	0.119	0.114	0.38	0.36
$p\sigma^3/\varepsilon$	0.14	0.15	0.30	0.31
$\langle N_1 \rangle$	0.044	*	1.61	2.0
$\langle N_2 \rangle$	35.2	108	111	108
$\langle U \rangle/N\varepsilon$	-1.16	-1.01	-3.08	-2.94

*Due to the very low value of N_1, this NpT simulation was done at infinite dilution.

uncertainity in $\langle N_i \rangle$ is rather large, especially when N_i is small. This leads to a large uncertainty in the calculated μ_i'/kT and makes comparing μ_i'/kT from μVT and NpT simulations difficult because in NpT simulations μ_i'/kT are directly calculated and are not subject to uncertainties in N_i. Since the residual values account for nonidealities and are the quantities of interest, it is unfortunate that we cannot directly specify μ_i'/kT in μVT simulations.

3.3 The effect of variation in BB_1

For a given solid solute 1, the chemical potential μ_1^c is primarily determined by the temperature, so varying BB_1 ($= \mu_1^c/kT + \ln(V/\sigma^3)$ at constant temperature does not correspond to any physically realizable changes in the system such as pressure variation or changing the solute (the same potential models are used). Since BB_1 is one of the prescribed parameters in the simulation, it would be useful to determine the consequence of varying its magnitude, so that when one wishes to optimize potential parameters to fit experimental data, the observed trends can be used as a guide. In Figure 2, we show the dependence of various observed quantities as a function of BB_1. BB_2, the chemical potential parameter of the solvent, is fixed at 3.35. The major trend observed is that the solubility of the solute $\langle N_1 \rangle$ increases with BB_1, the solute chemical potential parameter. This is the expected behavior for most mixtures. The increase in BB_1 also significantly increases the solvent concentration $\langle N_2 \rangle$ and hence the density, internal energy, and pressure of the mixture. This observed significant dependence of the concentration of one component on the chemical potential of another component is characteristic of fluids close to critical points.

3.4 The effect of varying BB_2

The primary effect of changing BB_2 is to vary the density of the mixture. Since the isotherm we chose is supercritical, varying BB_2 continuously changes the density from gas-like to liquid-like densities. In Figure 3, we show a plot of $\langle N_1 \rangle$ and $\langle N_2 \rangle$ versus BB_2 for $BB_1 = -5.6$. First we observe that $\langle N_2 \rangle$, the solvent density, increases very rapidly from a low value of less than 50 (corresponding to reduced density of about 0.16, a gas-like density) to about 150 ($\varrho^* = 0.48$, above critical density, or liquid-like density) over the BB_2 range of 3.2 to 3.4. Beyond BB_2 of 3.4, $\langle N_2 \rangle$ increases very slowly, due to the reduced compressibility of a liquid-like fluid. We already observed in Section 3.3 that changing the chemical potential of one component also affects the concentration of other components present. Similarly here, $\langle N_1 \rangle$ increases with BB_2 up to $BB_2 = 3.4$. Unlike $\langle N_2 \rangle$ which continues to increase, the observed $\langle N_1 \rangle$ reaches a peak, after which it drops rapidly. The decreasing portion of $\langle N_1 \rangle$ in Figure 3 is shown as a dotted line because this is not representative of real behavior. In real systems, $\langle N_1 \rangle$ behaves exactly like $\langle N_2 \rangle$, showing a gradual increase in this region and ultimately reaching a maximum at quite high densities (corresponding to a situation where molecules are so close together that the average pair interaction is repulsive) [9].

The maximum in $\langle N_1 \rangle$ observed here is indicative of the failure of the GCEMC technique to adequately sample concentration fluctuations in the dense fluid region [4]. This failure is much more pronounced and occurs at lower densities for the solute than for the solvent because the solute here is a much larger molecule and attempts to add or remove solute molecules become extremely difficult as the density of the

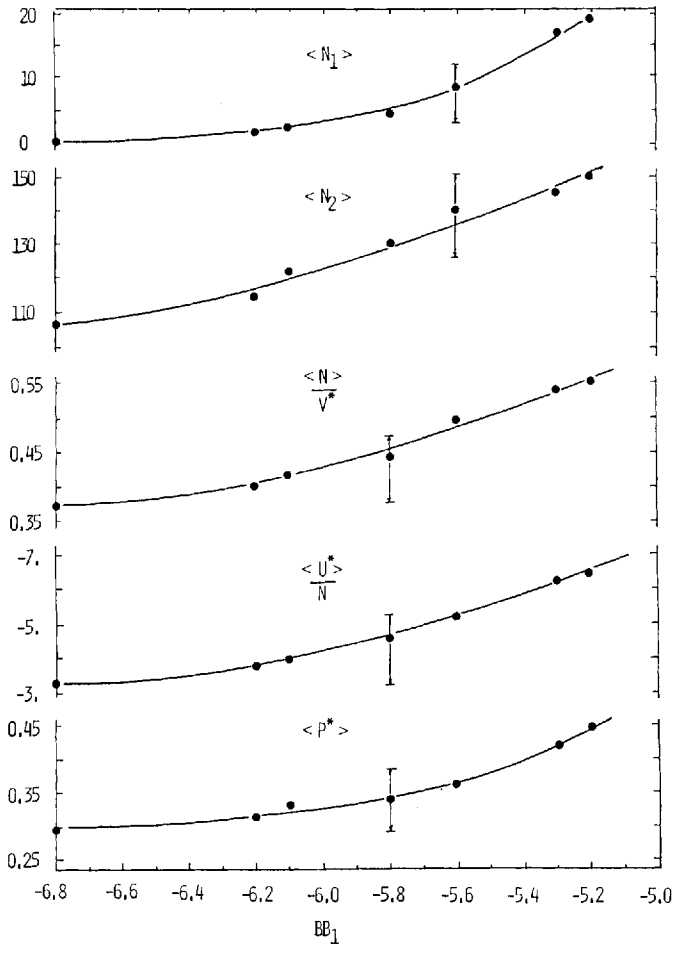

Figure 2 Effect of varying the solute chemical potential parameter $BB_1 \equiv \mu_1^r/kT + \ln\langle N_1 \rangle$. $BB_2 = 3.35$, $V/\sigma^3 = 305$.

system increases. This can be seen by examining equations (4) and (5). When i is a large molecule and when the system density is moderate to high, both ΔU^- and ΔU^+ tend to be large and positive. As a result, the addition/removal probability is nearly zero and dominated by the $\Delta U^{\pm}/kT$ term, the $\pm BB_i$ term is irrelevant. Physically, this means that, first of all, N_i no longer changes and the grand canonical ensemble has degenerated into a canonical ensemble. Also, because the specified BB_i values are irrelevant, the observed density and concentrations do not correspond to the specified chemical potentials. In Figure 3, we see indeed that while the fluctuations in N_1 and N_2 are quite large close to the critical region ($BB_2 = 3.1$–3.4), they become very small for $BB_2 > 3.5$. Therefore, in GCEMC simulations, small concentration fluctuations may be an indication that the method no longer works and the averages obtained are artificial. We note also that the artificial values of $\langle N_1 \rangle$ shown along the dotted part of the curve depend on the initial configuration of the simulation, particularly on the

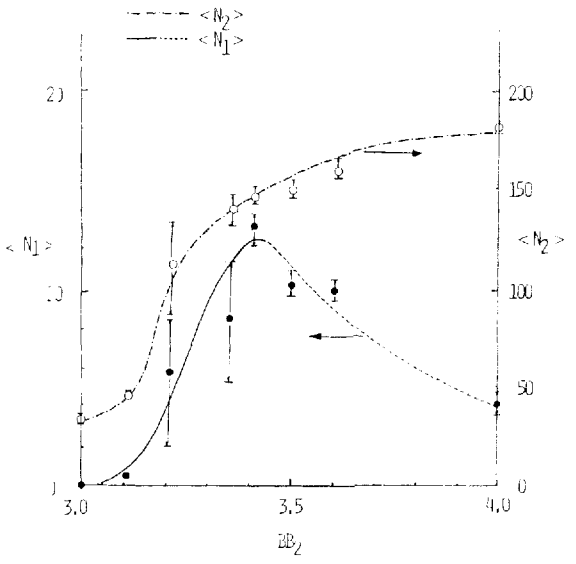

Figure 3 Effect of varying the solvent chemical potential parameter $BB_2 \equiv \mu_2^*/kT + \ln\langle N_2\rangle$. $BB_1 = -5.6$, $V/\sigma^3 = 305$.

value of N_1 at the beginning of the simulation. In our simulations, we always started with $N_1 = 0$ and allow the GCEMC sampling to reach the equilibrium value of $\langle N_1\rangle$. For the mixture we studied, GCEMC cannot be used when the reduced density exceeds about 1.5 times the critical density [10].

3.5 The effect of system size

In order to study the system-size dependence of GCEMC for our mixtures, we performed parallel simulations using 3 different values of volume V for a representative state condition. The values of V were chosen so that the 3 simulations contained approximately 30, 150 and 300 molecules respectively. The results are shown in Table 3. We see that the fluctuation magnitude relative to the mean value decreases with

Table 3 System size dependence $\langle N\rangle = \langle N_1\rangle + \langle N_2\rangle$

V/σ^3	64.9	301	531
μ_1^*/kT	−11.3	−11.3	−11.3
μ_2^*/kT	−2.36	−2.36	−2.36
$\varrho^* = \frac{\langle N\rangle}{V}\sigma^3$	0.49 ± 0.05	0.49 ± 0.04	0.50 ± 0.04
$\langle N_1\rangle$	2.6 ± 2	8.9 ± 4	15.9 ± 7
$\langle N_2\rangle$	29.2 ± 5	139 ± 13	249 ± 18
$p\sigma^3/\varepsilon$	0.78 ± 0.20	0.35 ± 0.09	0.35 ± 0.07
$\langle U\rangle/\langle N\rangle\varepsilon$	−5.9 ± 1.4	−5.3 ± 1.2	−5.4 ± 1.0
$y_1 = \frac{\langle N_1\rangle}{\langle N\rangle}$	0.08 ± 0.08	0.06 ± 0.04	0.06 ± 0.03

system size as we would expect. The pressure and solute concentration are most sensitive to system size. This is understandable because we have observed previously that the solubility is very sensitive to density fluctuations which are more restricted in small systems. The pressure is sensitive to V because it is calculated from the virial expression and is related to the derivative of the potential and hence converges more slowly than the internal energy. The tail correction for pressure is also more significant than that for U. For the properties we studied here, the system size dependence is not significant as long as the average N exceeds about 150.

3.6 The effect of addition of water

We investigated the effect of addition of a trace amount of water on the solute solubility. Two sets of simulations were performed, one set at a starting density below the critical density and the second set starting at above the critical density. One and two molecules of water were added to the mixtures at constant BB_1 and BB_2. In Table 4, we show the results for the first set of simulations. We see that with the addition of one molecule of water, there is a slight increase in the overall density and solute solubility. With the addition of a second molecule of water, there is a very large increase in density and a very dramatic increase in the solubility from about $y_1 = 0.005$ to $y_1 = 0.10$. This dramatic increase in solubility is closely related to the high compressibility of the mixture near the critical density. The fact that the system is near the critical point can be deduced from the much larger statistical fluctuations observed when two water molecules are added. The addition of a highly polar molecule such as water interacts strongly with the solvent CO_2 and solute naphthalene, both of which are quadrupolar. The strong interactions result in an increase in the cohesive energy of the mixture and a large density increase which in turn induce a higher solubility .

It is somewhat surprising that the addition of the first water molecule had such little effect, while the addition of the second molecule resulted in a dramatic solubility increase. Our speculation is that having only a single H_2O molecule in the volume is essentially similar to a situation in which H_2O is present at infinite dilution. In such cases there can be no preferential aggregation of H_2O molecules, which may be important in the near critical region. (Molecular aggregation effects are discussed in more detail in Section 3.7 where distribution functions are shown). When more than one water molecule is present, they tend to aggregate due to strong dipolar inter-

Table 4 Effect of water addition at below critical density. $V/\sigma^3 = 305$, $\langle N\rangle = \langle N_1\rangle + \langle N_2\rangle + N_{H_2O}$

BB_1	-5.0	-5.0	-5.0
BB_2	3.1	3.1	3.1
N_{H_2O}	0	1	2
$\varrho^* = \frac{\langle N\rangle}{V}\sigma^3$	0.15 ± 0.01	0.16 ± 0.01	0.35 ± 0.25
$\langle N_1\rangle$	0.17 ± 0.03	0.23 ± 0.04	10.6 ± 8.4
$\langle N_2\rangle$	44.7 ± 3.2	46.4 ± 3.5	92.8 ± 30.5
$p\sigma^3/\varepsilon$	0.18 ± 0.01	0.18 ± 0.01	0.23 ± 0.12
$\langle U\rangle/\langle N\rangle\varepsilon$	-1.47 ± 0.12	-1.63 ± 0.15	-3.37 ± 2.0
$y_1 = \frac{\langle N_1\rangle}{\langle N\rangle}$	0.0038	0.0048	0.10

actions; thus, local regions of relatively higher densities are created where further addition of solute is favored. The water aggregates can be regarded as "sites" where the solutes can "condense".

Another reason that adding one single water molecule has little effect is that the starting density (about $\varrho^* = 0.18$) is probably too low compared to the critical density, so that one single H_2O molecule does not provide sufficient cohesive energy to draw molecules close together. We suspect that if the starting density were closer to, but below, the critical value, a single H_2O molecule might be sufficient to cause a dramatic effect as well. This dependence on starting density is further illustrated in Table 5 where one and two H_2O molecules are again added to a CO_2/naphthalene mixture, but now the starting density is $\varrho^* = 0.42$, which is higher than the critical density of the solvent. We see that the addition of H_2O increases the solubility as one would expect, but the effect is undramatic. The overall density is also only slightly increased. We note that the values of BB_1 used in the two sets of simulations shown in Tables 4 and 5 are different. A higher value (corresponding to a more soluble solute) was used for the lower density set (Table 4) so that the solubility is not too low and meaningful values of $\langle N_1 \rangle$ could be obtained.

3.7 *Distribution Functions – molecular aggregation*

We have attributed the variation of solubility, fluctuations and the effect of water addition to the presence of local density variations. When the average density is subcritical and the temperature is slightly supercritical, the addition of a highly polar molecule such as water attracts the solvent and solute molecules strongly and creates a local high-density environment in its vicinity. This favors addition of more solute and a high local solubility results. Therefore, aggregation of solute about water molecules serves to stablize the large solute molecules in the supercritical phase. Such local preferential aggregations of solutes and solvents can be seen from studying the distribution functions obtained from the simulations. We show here only a few typical plots.

Figure 4 shows the CO_2-CO_2 radial distribution function g_{22} which is typical of moderately dense fluids and is given for comparison purposes. The only point to note is that the first peak is about 2 and occurs at approximately $r^* = 1.1$. For the CO_2-napthalene radial distribution function g_{12}, the first peak is higher, indicating

Table 5 Effect of water addition at about critical density $V/\sigma^3 = 305$, $\langle N \rangle = \langle N_1 \rangle + \langle N_2 \rangle + N_{H_2O}$

BB_1	6.1	−6.1	−6.1
BB_2	3.35	3.35	3.35
N_{H_2O}	0	1	2
$\varrho^* = \frac{\langle N \rangle}{V}\sigma^3$	0.42 ± 0.05	0.45 ± 0.05	0.46 ± 0.06
$\langle N_1 \rangle$	2.4 ± 2.0	3.5 ± 2.7	4.3 ± 3.0
$\langle N_2 \rangle$	122 ± 15	130 ± 13	130 ± 15
$p\sigma^3/\varepsilon$	0.33 ± 0.08	0.32 ± 0.08	0.34 ± 0.09
$\langle U \rangle / \langle N \rangle \varepsilon$	−4.0 ± 1.2	−4.4 ± 1.3	−4.6 ± 1.4
$y_1 = \frac{\langle N_1 \rangle}{\langle N \rangle}$	0.019	0.026	0.032

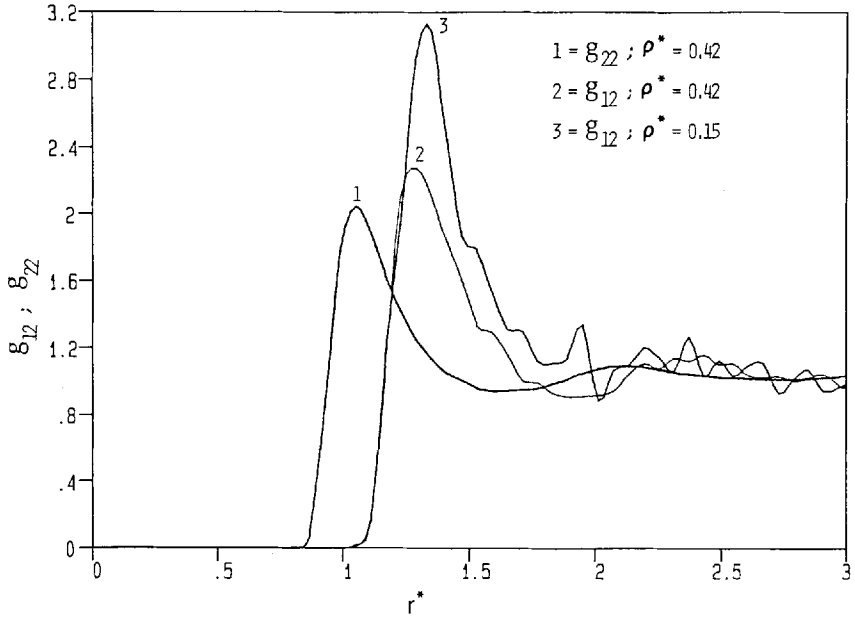

Figure 4 Typical CO_2-CO_2 radial distribution function g_{22} and CO_2-naphthalene radial distribution function g_{12}. $BB_1 = -6.1$, $BB_2 = 3.35$, $V/\sigma^3 = 305$.

CO_2 molecules are drawn closer to solute naphthalene, due to the stronger interactions. The first peak in g_{12} for the low density case ($BB_2 = 3.1$, $\varrho^* = 0.15$) is higher than that for the higher density case ($BB_2 = 3.35$, ϱ^* 0.42), because the increase in local density due to presence of solute is more pronounced at low densities due to higher compressibility.

The naphthalene-naphthalene radial distribution functions shown in Figure 5 indicate that, first of all, there is a strong tendency for the napthalene molecules to pair up and the first peak is now quite high (about 4.5). Furthermore, there seems to be a secondary peak at about $r^* = 1.6$, corresponding to the presence of triplets and larger aggregates. This secondary peak is diminished when water is added because H_2O is also a strongly interacting molecule and the naphthalene molecules can now aggregate around the H_2O molecules as well as around other naphthalene molecules.

The effect of H_2O is further illustrated in Figure 6 where the H_2O-naphthalene radial distribution functions g_{13} are shown. The fact that the solute napthalene molecules are strongly attracted to H_2O and tend to aggregate around H_2O is indicated by the very large first peak. Again, the first peak is reduced when more water is added because there is now more competition for the naphthalene molecules since they can choose to aggregate around any of the H_2O molecules present. The trends shown by g_{11} and g_{13} should be considered as qualitative only, because the statistics are not too good since both naphthalene and H_2O are present in low concentrations. Unless very large systems or very long simulations are used, there is little one can do to significantly improve the statistics. Despite the poor statistics similar qualitative trends are observed in other simulations carried out in this study.

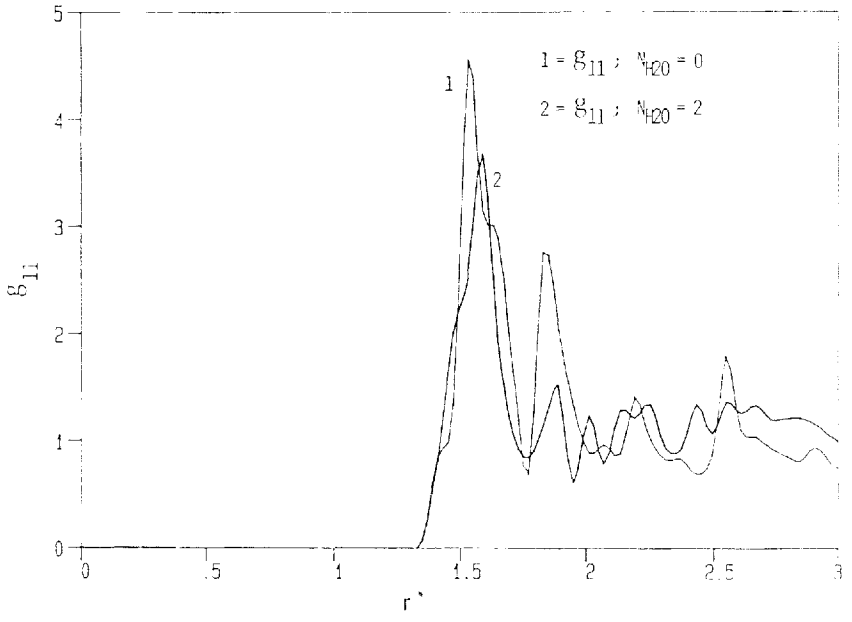

Figure 5 Naphthalene-naphthalene radial distributon functions g_{11} with and without water. State condition as for Figure 4.

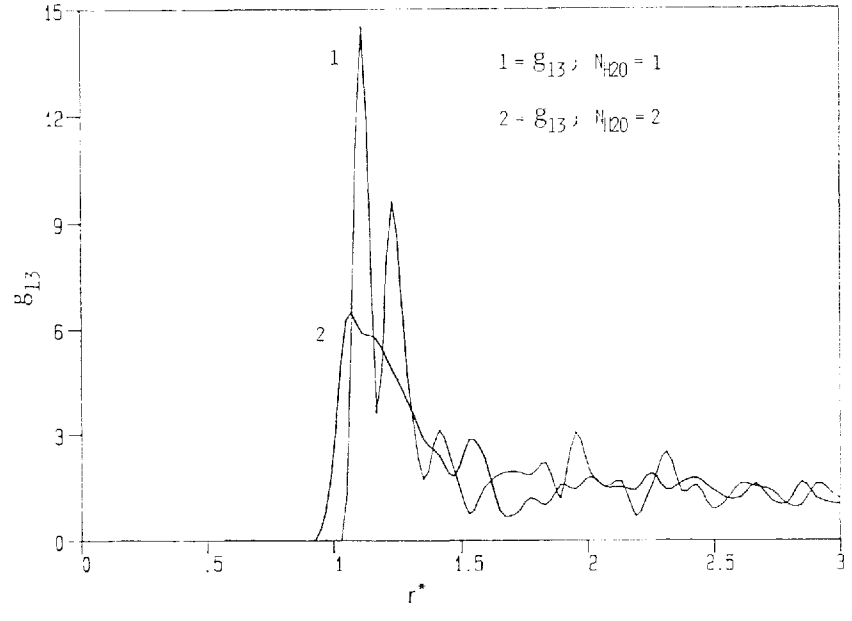

Figure 6 Water-naphthalene radial distribution functions g_{13}. State condition as for Figure 4.

4. CONCLUSIONS

GCEMC simulations for highly nonideal mixtures can be carried out in the near critical region. The results are in agreement with those obtained from NpT simulations within the statistical uncertainties. The GCEMC method has the advantage of allowing specification of the configurational chemical potentials μ_i^c at the beginning of the simulation; however, due to the rather large statistical uncertainties in $\langle N_i \rangle$, the residual chemical potentials, which are direct measures of nonidealities, cannot be obtained with high precision. The GCEMC method also permits density and concentration fluctuations. These fluctuations are found to be large and highly correlated in the near critical region; therefore, artificial suppression of these fluctuations in one component of the mixture (by fixing one of the N_i in the system for example) in a finite-size system may lead to erroneous results.

In our system, we found that changing the chemical potential μ_i^c of any component i, while keeping the other chemical potentials constant, affects not only the concentration of that particular component, but significantly changes the concentration of all other components present as well. This is a result of the strong interactions between solute and solvent molecules as well as the fact that the state conditions are near critical. Such features are typical of supercritical extraction systems. Unfortunately, this also means that a certain amount of trial and error is necessary in selecting the appropriate combination of chemical potentials and volume to simulate the physical state of interest.

The solubility of the naphthalene was found to be strongly dependent on density and increases rapidly as the system density increased from a gas-like value, in agreement with other simulation studies and experimental results. The observed solubility exhibited an artificial decline at moderately high density due to the failure of the GCEMC method to sample density and concentration fluctuations adequately. Four our system, this failure occurred when the density reached about $\varrho^* = 0.55, 1.5$ times the solvent critical density. When a small amount of a highly polar molecule such as water was added to the system, the solubility was increased due to favorable interactions between water and solute. The increase in solubility was relatively small if the system density before water addition was near or higher than critical because the mixture compressibility was low. If the density before water addition was low compared to the critical density, the observed increase in solubility due to water addition was very dramatic. This dramatic solubility enhancement is the result of a combination of several factors: the high compressibility of the mixture in the near critical region, and the ability of the strongly polar water molecules to attract solute molecules around it to form stable aggregates. The tendency of the solute and water molecules to aggregate was clearly demonstrated in the radial distribution functions, where large and broad peaks were observed in the naphthalene-naphthalene and water-naphthalene distribution functions. This direct link between fluid structure at the molecular level and observed solubility behavior makes molecular simulation a very powerful tool in mixture studies.

Acknowledgement

Support by the National Science Foundation under Grant CBT 8452001 is acknowledged. Support by the SDSC is also acknowledged.

References

[1] G.M. Schneider, E. Stahl, G. Wilke, *Extraction with Supercritical Gases*, Verlag Chemie, Weinheim, 1980; M.E. Paulaitis, J.M. Penninger, R.D. Gray, Jr., P. Davidson, *Chemical Engineering at Supercritical Conditions*, Ann Arbor Science, Ann Arbor, MI, 1983; M.A. McHugh, V.J. Krukonis, *Supercritical Fluid Extraction, Principle and Practice*, Butterworth, London, 1986.

[2] K.S. Shing and S.T. Chung, "Computer Simulation Methods for the Calculation of Solubility in Supercritical Extraction Systems", *J. Phys. Chem.*, **91,** 1674 (1987).

[3] J.M. Dobbs and K.P. Johnston, "Selectivities in Pure and Mixed Supercritical Fluid solvents", *Ind. Eng. Chem. Res.* **26,** 1476 (1987).

[4] D.J. Adams, "Chemical Potential of Hard-sphere Fluids by Monte Carlo Methods", *Mol. Phys.* **28,** 1241 (1974); D.J. Adams "Grandcanonical Ensemble Monte Carlo for a Lennard-Jones Fluid", *Mol. Phys.* **29,** 307 (1975).

[5] C.G. Gray and K.E. Gubbins, *Theory of Molecular Fluids*, Appendix D, Oxford University Press, 1984.

[6] H. Margenau and N.R. Kestner, *Theory of Intermolecular Forces*, McGraw-Hill, New York, 1971.

[7] T.M. Reed and K.E. Gubbins, *Applied Statistical Mechanics*, McGraw-Hill, New York, 1973 Chap. 3.

[8] S.T. Chung, "A Study of Supercritical Fluid Extraction", M.S. Thesis, University of Southern California (1986); S.T. Chung, Private Communications.

[9] J.J. Czubryt, M.N. Meyers and J.C. Gidding, "Solubility Phenomena in Dense Carbon-Dioxide Gas in the Range 270–1900 Atmospheres", *J. Phys. Chem.* **74** 4260 (1970).

[10] There are simulation techniques designed to overcome partially this problem. An example is the cavity biased method of M. Mezei, "A Cavity Biased (T, V, μ) Monte Carlo Method for the Computer Simulation of Fluids", *Mol. Phys.* **40,** 901 (1980). When the solute is large compared to solvent, such methods are not effective.